# Low-Lying Energy Properties of a Frustrated Antiferromagnetic Spin-$\frac{1}{2}$ Ladder

Xiaoqun Wang
*Institut Romand de Recherche Numérique en Physique des Matériaux, PPH-EPFL, CH-1015 Lausanne, Switzerland*
(February 1, 2008)

## Abstract

Using the Density Matrix Renormalization Group method, we determined the phase diagram of a frustrated antiferromagnetic spin-$\frac{1}{2}$ ladder at zero temperature. Two spin-gapped phases, the Haldane phase and the singlet phase, are identified. A phase transition between the two phases occurs at any non-zero value of frustration coupling $J_\times$. On the phase boundary, the spin gap vanishes for sufficiently small $J_\times$. Crossing this non-gapped line, the transition is of second order, while of first order for larger $J_\times$. Striking frustration effects are predicted for ladder materials.

PACS. 75.10.Jm, 75.30.Kz, 75.45.+j

In recent years, a lot of theoretical and experimental effort has been devoted to the understanding of spin-$\frac{1}{2}$ antiferromagnetic ladders. [1–9] These systems, which interpolate structures between one and two dimensions, are realized in materials such as $Sr_{n-1}Cu_{n+1}O_{2n}$ [1]. The ladders, being arrays of coupled chains, can display significantly different physical properties according to their number of legs. Especially, the spin correlation function in the ground state shows an algebraic decay if the number of legs is odd and an exponential decay if it is even. [4,7] This property essentially depends on whether or not the system exhibits a *spin gap* in the spectrum. Therefore, it seems that the ladders are analogous to spin-$S$ antiferromagnetic Heisenberg chains where an odd half-integer spin corresponds to an odd number of legs and an integer spin to an even number of legs. [10–15]

The aim of this paper is to investigate the following two issues: i) How far is the above analogy valid? In particular, are the low-lying energy properties of the two-leg standard ladder identical to those of the single $S = 1$ chain? It is clear that a two-leg ladder with a ferromagnetic interchain coupling $J_\perp < 0$ is equivalent to the $S = 1$ chain when $J_\perp \to -\infty$. In the case of the antiferromagnetic interchain coupling, there is also a gap opening at any $J_\perp$, however no phase transition occurs in the whole parameter range. [16]. For large $J_\perp$, the gap stems from the formation of a spin singlet on each rung. Therefore the origin of the spin gap for $J_\perp > 0$ seems distinguishable from that in the $S = 1$ chain. [1] ii) What are the frustration effects caused by a next-nearest-neighbour interaction $J_\times$? Under some circumstances, frustration can produce either a dimerized state or a non-dimerized spin liquid state. [17] In the ladder material $SrCu_2O_3$, [9] the frustration is presumed to be negligible and $J_\perp$ comparable to the intrachain coupling $J_\parallel$. [1] In this case, compared to the theoretical prediction of $\Delta = 0.5J_\parallel$ [2,4], the gap is estimated 35% smaller by fitting the spin susceptibility and 4% larger from the nuclear magnetic resonance measurement. [9] The origin of this discrepancy between the two estimates is unclear. [1] Our calculation will show that for $J_\perp = J_\parallel$ the spin gap only slightly changes as $0 \le J_\times \le 0.4J_\parallel$. The maximum value of $\Delta$ is $0.519J_\parallel$ at $J_\times = 0.25J_\parallel$. Therefore, it is an open question whether ladder materials are sufficiently well described by the standard spin ladder.

In this work, we study a two-leg frustrated antiferromagnetic spin-$\frac{1}{2}$ ladder described by:

$$\begin{aligned}\hat{H} = \sum_{i=1,N} & [J_\parallel(\hat{\mathbf{S}}_{1,i}\cdot\hat{\mathbf{S}}_{1,i+1} + \hat{\mathbf{S}}_{2,i}\cdot\hat{\mathbf{S}}_{2,i+1}) + J_\perp\hat{\mathbf{S}}_{1,i}\cdot\hat{\mathbf{S}}_{2,i} \\ + & \quad J_\times(\hat{\mathbf{S}}_{1,i}\cdot\hat{\mathbf{S}}_{2,i+1} + \hat{\mathbf{S}}_{1,i+1}\cdot\hat{\mathbf{S}}_{2,i})], \end{aligned} \tag{1}$$

where $\hat{\mathbf{S}}_{n,i}$ denotes a spin-$\frac{1}{2}$ operator at site $i$ of the $n$th chain. $J_\parallel$ is an intrachain coupling between two neighboring spins in each chain, $J_\perp$ an interchain coupling between two spins on each rung and $J_\times$ an interchain coupling between two spins of neighboring rungs. Since $J_\times = J_\parallel$ is a symmetric line in the parameter space, we only consider the case of $J_\times \le J_\parallel$. When $J_\times = 0$, $\hat{H}$ reduces to that for the standard spin ladder. Hereafter we set $J_\parallel = 1$.

To overcome the inherent difficulties related to the frustration, which plague the Monte Carlo simulation, we employ the density matrix renormalization group method invented by White. [18] This method has proven to be very powerful and efficient for a systematic study of low-lying energy properties of low-dimensional lattice models. In our calculation, we keep at least 240 states, and up to 450 states are necessary for critical regimes. The truncation error is typically of the order of $10^{-8}$. Lengths up to 550 rungs are considered for open boundary conditions and finite size scaling is used to determine the thermodynamic limit.

For convenience, the number of rungs $N$ is chosen to be even. To check the accuracy and the convergence, we performed calculations keeping up to 600 states. The errors on physical quantities are estimated to be less than one percent in most cases. The technical details will be given elsewhere. [19]

In Fig. 1, we show the phase diagram characterized by two fixed points: (i) the "Haldane phase" so named as it contains the limiting case $J_\times = 1$ and $J_\perp = 0$,

$$\hat{H} = \sum (\hat{\mathbf{S}}_{1,i} + \hat{\mathbf{S}}_{2,i}) \cdot (\hat{\mathbf{S}}_{1,i+1} + \hat{\mathbf{S}}_{2,i+1}) \tag{2}$$

whose low-lying spectrum is identical to that of a $S = 1$ chain; (ii) the "singlet phase" as it contains the case $J_\perp \gg 1$, with a ground state consisting of a singlet on each rung and low-lying excitations generated by creating triplets on rungs. In both cases, the system is gapped. However, a phase transition (shown in Figs. 3-5) occurs in the parameter space as we cross from (i) to (ii).

Of special interest in the characterization of the two phases, is the sensitivity of their low-lying energy spectra to boundary conditions or impurity effects. In particular, both experiment [20] and numerical calculations [21,22] indicate that boundary or impurity effects are a characteristic feature of the $S = 1$ chain [23].

In the *Haldane phase*, for open boundary conditions, the ground state is four-fold degenerate with total spin $S_t = 0, 1$ and the continuum starts with $S_t = 2$ as shown schematically in Fig. $2a_o$, while for periodic boundary conditions, the ground state becomes a singlet and the lowest excitation has $S_t = 1$ (Fig. $2a_p$). We can understand this difference by considering the open boundary conditions as a special case of a bond impurity in the weak or strong coupling limit [22,24].

Furthermore, for open boundary conditions only, the region $C_1$ appears inside the Haldane phase, characterized by the presence of midgap states. The number of levels is one as we enter the $C_1$ region from below (Fig. 2b) and grows larger and larger as we approach the phase boundary (Fig. 2c). This effect is a peculiar feature of this frustrated spin ladder in contrast to the $S = 1$ chain.

In the *singlet phase*, independently of the boundary conditions, the ground state is a singlet and the continuum starts from a state with $S_t = 1$ outside the region $C_2$ and $S_t = 0$ inside the region $C_2$ (Fig. 2d-f). In contrast to the Haldane phase, neither midgap states for open boundary conditions nor any impurity state due to a bond impurity are found in this phase. [24]

On the *phase boundary*, there are at least three non-trivial degenerate states. Two of them have $S_t = 0$ and one has $S_t = 1$. As $J_\times \leq \lambda = 0.287$, a non-gapped line shows up on the boundary curve (Fig. 2g). Below we will discuss the phase diagram as it is numerically determined by the calculation of the ground state energy, singlet density per rung and low-lying excitations.

Fig. 3 shows the ground state energy per rung $e_0$. For each $J_\times$, a phase transition between the Haldane phase (left) and the singlet phase (right) takes place at the maximum value of $e_0$. When $J_\times$ is sufficiently large, $e_0$ is obviously singular at the critical value of $J_\perp$. When $J_\times = 1$, the singularity originates from the crossing of the two lowest energy levels with $S_t = 0$. However, such a crossing *disappears* due to *level repulsion* for $J_\times < 1$. The two lowest energy levels with $S_t = 0$ become degenerate at the critical values *only* in the thermodynamic limit. When $J_\times$ is small, the curvature of $e_0$ looks smooth at its maximum

value. The critical values $J_{\perp,0}$ of $J_\perp$ are given in Table I, which are splined into a solid curve to indicate the phase boundary shown in Fig. 1. In the construction of the phase diagram, we also verified the transition by varying $J_\times$ for given $J_\perp$. The results for $J_\perp = 1$ is shown in inset.

In order to further investigate the ground state properties, we calculate the singlet density per rung $\rho_s$. For a state $|\Psi\rangle$, we define $\rho_s = \frac{1}{N}\sum_i \langle\Psi|\mathcal{S}_i\mathcal{S}_i^\dagger|\Psi\rangle$, where $\mathcal{S}_i = \frac{1}{\sqrt{2}}(|\uparrow_1\downarrow_2\rangle_i - |\downarrow_1\uparrow_2\rangle_i)$ is the singlet state formed by two spins on the $i$th rung. For $J_\times = 1$ and in low-lying energy states, $\rho_s = 1$ when $J_\perp > J_{\perp,0}$; otherwise $\rho_s = 0$. For $J_\times < 1$, we show $\rho_s$ for the ground state in Fig. 4. At $J_{\perp,0}$, $\rho_s$ changes abruptly for large $J_\times$ and smoothly for small $J_\times$. We note that $\rho_s = \frac{1}{4}$ at $J_\perp = J_\times = 0$, $\rho_s < \frac{1}{4}$ in the Haldane phase, and $\rho_s > \frac{1}{4}$ in the singlet phase. Therefore, $\rho_s$ also characterizes all the phases.

We now discuss the low-lying excitations which are used to determine the regions $C_1$ and $C_2$ as well as to provide evidence for the existence of a non-gapped line. The spin gap $\Delta$ governs the asymptotic behavior of the correlation function in the ground state and the low-temperature behavior of the thermodynamic quantities. $\Delta$ is defined as an energy difference between the ground state and the bottom state of continuum for spin systems. In Fig. 5, we show the energies of several relevant states relative to the ground state energy.

For $J_\times = 1$, the total spin on each rung is conserved. Consequently, the states with $n$-singlets on rungs are the same as those of a $S = 1$ chain doped by $n$ non-magnetic impurities at sites corresponding to those rungs at which the $n$-singlets are localized. In the Haldane phase, the midgap states are the lowest impurity states for the given number of singlets or impurities. For instance, two lowest midgap states shown in inset are the ground states of open $S = 1$ chains with $N-1$ and $N-2$ spins: the lowest one involves a singlet at one end of an open ladder and the other two singlets at both ends. In the singlet phase, the low-lying excitations are discrete but infinitely degenerate. Two lowest excitations shown in inset are generated from the ground state by introducing one, two, and four neighbouring triplets on rungs. Their $S_t$ equal to one when one triplet is involved, or else $S_t = 0$.

For $J_\times < 1$, since the total spin on each rung is no longer conserved, the low-lying energy properties are dramatically changed according to the magnitude of $J_\times$ and $J_\perp$. As shown in Fig. 5, there is no midgap state at $J_\times = 0.2$ and 0.4. For a larger $J_\times$, midgap states show up when $J_\perp$ is larger than a critical value $J_{\perp,1}$. Splining $J_\times$ and $J_{\perp,1}$ given in Table I, we obtained a critical values for $J_\times$ of 0.430. In the singlet phase, the infinite degeneracy at $J_\times = 1$ is removed by infinitesimal $J_\parallel - J_\times$ so that the discrete levels become different bands. The bottom state has $S_t$ equal to 1 or 0 depnding on $J_\times$ and $J_\perp$. For sufficiently large $J_\times$, the two lowest excitations with $S_t = 0, 1$ across at $J_\perp = J_{\perp,2}$. Several $J_{\perp,2}$ given in Table I are used to determine the value of $J_\times$, namely $\lambda = 0.287$, at which the splined curve meets the phase boundary. We note that this leads to a critical point in the phase diagram because the splined curve has a curvature clearly opposite to that of the phase boundary.

As seen from Fig. 5, for each $J_\times < 1$ the spin gap has a minimum given in Table I at $J_{\perp,0}^-$. For sufficiently large $J_\times$, $\Delta$ has a jump at $J_{\perp,0}$, e.g. see Fig. 5 for $J_\times = 0.8$. We found that the *jump* and the *minimum value*, and the *width* of $C_2$ decrease coherently as $J_\times$ becomes small and *approach to zero* for $J_\times \to \lambda$. Therefore, a non-gapped line exists on the phase boundary for $0 \le J_\times \le \lambda$. On this line, $\rho_s = 1/4$ and the ground state has a different symmetry than in the other phases. [19] Further taking into account the critical behavior of $e_0$ and $\rho_s$, we conclude that the transition between the Haldane phase and the singlet phase

crossing the non-gapped line is of second order, while of first order for $J_\times > \lambda$.

In Fig. 6, we show the behavior of the spin gap varying $J_\times$ for $J_\perp = J_\parallel = 1$, as is relevant to ladder materials such as $SrCu_2O_3$, [1] It is remarkable that the spin gap is almost constant when $0 \leq J_\times \leq 0.4$. At $J_\times = 0.25$, it has a maximum value of $\Delta = 0.519$. Accordingly, it would be interesting to examine the relevance of frustration in ladder materials.

We have established the phase diagram of a frustrated spin-$\frac{1}{2}$ ladder using the low-lying energy properties. Clearly, the low-lying energy properties of the two-leg antiferromagnetic spin-$\frac{1}{2}$ ladder is different from those of the $S = 1$ chain. According to our findings, one can naturally expect similar effects for a frustrated $t - J$ ladder. In addition, for very low carrier doping, bound states should occur in the Haldane gap. As far as materials are concerned, it would be interesting to explore two kinds of impurity effects: non-magnetic and magnetic doping, which produce midgap states for sufficiently large value of $J_\times$ and impurity states for any non-zero value of $J_\times$ in the Haldane gap, respectively. Moreover, in order to observe the phase transition, one could measure the specific heat and spin susceptibility on pure ladder materials for different interchain coupling.

The author is very grateful to Martin Long, Felix Naef and Xenophon Zotos for their kind help and stimulating discussions. He also thanks A. Honecker, I. Peschel, and Y. Zhao for discussions. This work is supported by the Swiss National Fond Grant No. 20-49486.96.

# REFERENCES


[1] E. Dagotto and T.M. Rice, Science, **271**, 618(1996).
[2] E. Dagotto, et al Phys. Rev. B **45**, 5744(1992).
[3] S.P. Strong aand A.J. Millis, Phys. Rev. Lett. **69**, 2419(1992).
[4] S.R. White, et al Phys. Rev. Lett. **73**, 886(1994).
[5] T.M. Rice, et al, Europhs. Lett. **23**, 445(1993); M. Sigrist, et al, Phys. Rev. B **49**, 12058(1994).
[6] M. Troyer, et al Phys. Rev. B **50**, 13515(1994).
[7] M. Greven, et al, Phys. Rev. Lett. **77**, 1865(1996).
[8] T. Barnes and J. Riera, Phys. Rev. B **50**, 6817(1994).
[9] M. Azuma *et al*, Phys. Rev. Lett. **73**, 3463(1994).
[10] F.D.M. Haldane, Phys. Lett. A**93**, 464(1983).
[11] S.R. White and D.A. Huse, Phys. Rev. B **48**, 3844(1993).
[12] O. Golinelli et al., Phys. Rev. B **50**, 3037(1994).
[13] K. Hallberg, et al Phys. Rev. Lett. **76**, 4955(1996).
[14] U. Schollwöck and Th. Jolicoeur, Europhys. Lett. **30**, 493)(1995).
[15] S. Qin, et al Phys. Rev. B. **56**, R14251(1997).
[16] S.R. White, Phys. Rev. B **53**, 52(1996).
[17] S.R. White and I. Affleck, Phys. Rev. B **54**, 9862(1996).
[18] S.R. White, Phys. Rev. Lett. **69**, 2863(1992).
[19] Xiaoqun Wang, unpublished.
[20] J.F. DiTusa et al, Phys. Rev. Lett. **73**, 1857(1994).
[21] T. Kennedy, J. Phys. Condens. Matter **2**, 5737(1990).
[22] X. Wang and S. Mallwitz, Phys. Rev. B **48**, R492(1996).
[23] The string order parameter alternatively distinguishes different spin-gapped phases for an anisotropic $S = 1$ chain. It is finite in the Haldane phase and vanishes in the large-$D$ phase. [25] However it is not uniquely defined for ladders. [16,26] If the definition of Refs. [16,26] is used for the anisotropic $S = 1$ chain which is maped into a frustrated ladder, this parameter does not vanishes in the large-$D$ phase (contradiction!). If the other definition is used, this parameter is finite in the Haldane phase and vanishes in the singlet and large-$D$ phases. [19]
[24] The nature of impurity states depends upon the manner of magnetic doping. Here a bond impurity means that the couplings $J'_\times \neq J_\times$ and $J'_\parallel \neq J_\parallel$ are introduced, due to local doping, for four spins in two neighboring rungs. [22] The detailed results will be given elsewhere [19].
[25] M. den Nijs and K. Rommelse, Phys. Rev. B **40**, 4709(1989); T. Kennedy and H. Tasaki, ibid **45**, 304(1992); R.Botet, et al, ibid **28**, 3914(1983); Y. Hatsugai and M. Kohmoto, ibid **44**, 11789(1991).
[26] Hiroshi Watanabe, Phys. Rev. B **52**,12508(1995).

## TABLES

TABLE I. For several values of $J_\times$, $J_{\perp,0}, J_{\perp,1}, J_{\perp,2}$ are the values of $J_\perp$ for points on the phase boundary, lower boundary of $C_1$ and upper boundary of $C_2$, respectively; $\Delta_{min}$ is the minimum of $\Delta$. Lower numbers are errors at the last digit.

| $J_\times$ | 0.2 | 0.35 | 0.4 | 0.5 | 0.6 | 0.8 | 1 |
|---|---|---|---|---|---|---|---|
| $J_{\perp,0}$ | $0.378_3$ | | $0.715_2$ | | $1.000_5$ | $1.225_5$ | 1.4015 |
| $J_{\perp,1}$ | | | | $0.792_8$ | $0.835_5$ | $0.917_5$ | 0.991 |
| $J_{\perp,2}$ | | $0.650_8$ | $0.742_8$ | $0.921_5$ | $1.118_3$ | $1.560_5$ | 2 |
| $\Delta_{min}$ | $0.004_4$ | | $0.027_5$ | | $0.130_5$ | $0.318_2$ | 0.4105 |

## FIGURES

FIG. 1. Phase diagram: a thick solid curve splining dots indicates the phase boundary; Dotted line the symmetric line; $C_1$ is surrounded by the phase boundary, a thin curve splining diamonds and the symmetric line; $C_2$ by the phase boundary, a thin curve splining squares and the symmetric line. Schematic spectra of points a–g are shown in Fig. 2.

FIG. 2. Schematic spectra for the points a–g of Fig. 1. Lines, shaded rectangles and numbers denote levels, the continuum and $S_t$ of the levels or the continuum, respectively.

FIG. 3. Ground state energy per rung $e_0$ *vs* $J_\perp$ at $J_\times$= 0,0.2,0.4,0.6,0.8, and 1. In inset, it *vs* $J_\times$ at $J_\perp = 1$.

FIG. 4. The singlet density per rung $\rho_s$ in the ground state *vs* $J_\perp$ at $J_\times = 0, 0.2, 0.4, 0.6$, and 0.8.

FIG. 5. Low-lying energies relative to the ground state energy *vs* $J_\perp$ and $J_\times$ for the open boundary condition. In the *Haldane phase*, solid triangles linked by solid lines indicate the bottom state of the continuum ($S_t = 2$). Squares linked by dashed lines the lowest midgap states (MS) ($S_t = 1$). In the *singlet phase*, triangles or dots linked by solid lines and diamonds linked by dashed lines denote the two lowest excitations with $S_t = 1, 0$, respectively. Inset for $J_\times = 1$.

FIG. 6. Spin gap *vs* $J_\times$ at $J_\perp = J_\parallel$

.

# Wang, Figure 1: phase diagram

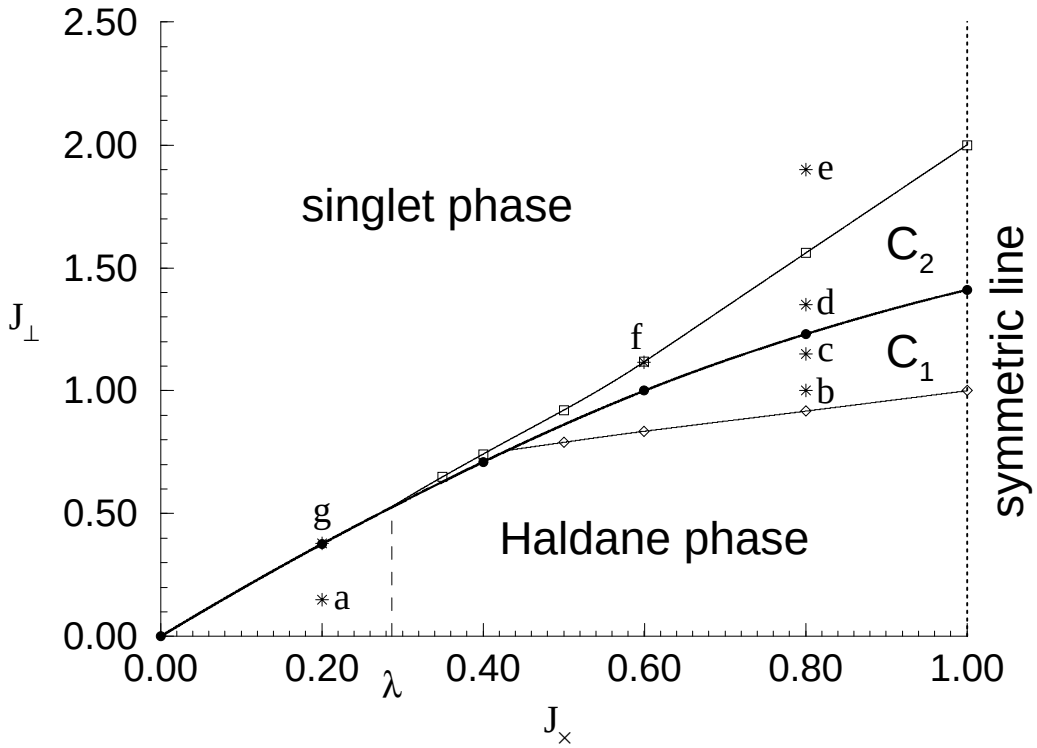

Wang, Figure 2: schematic spectrums

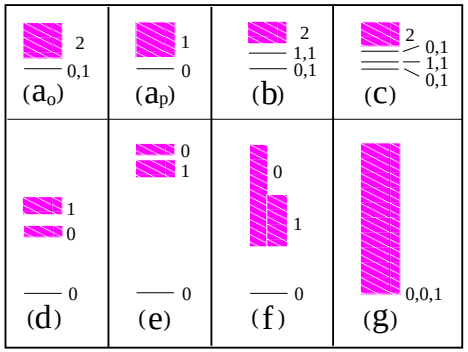

Wang, Figure 3: ground state energy per rung

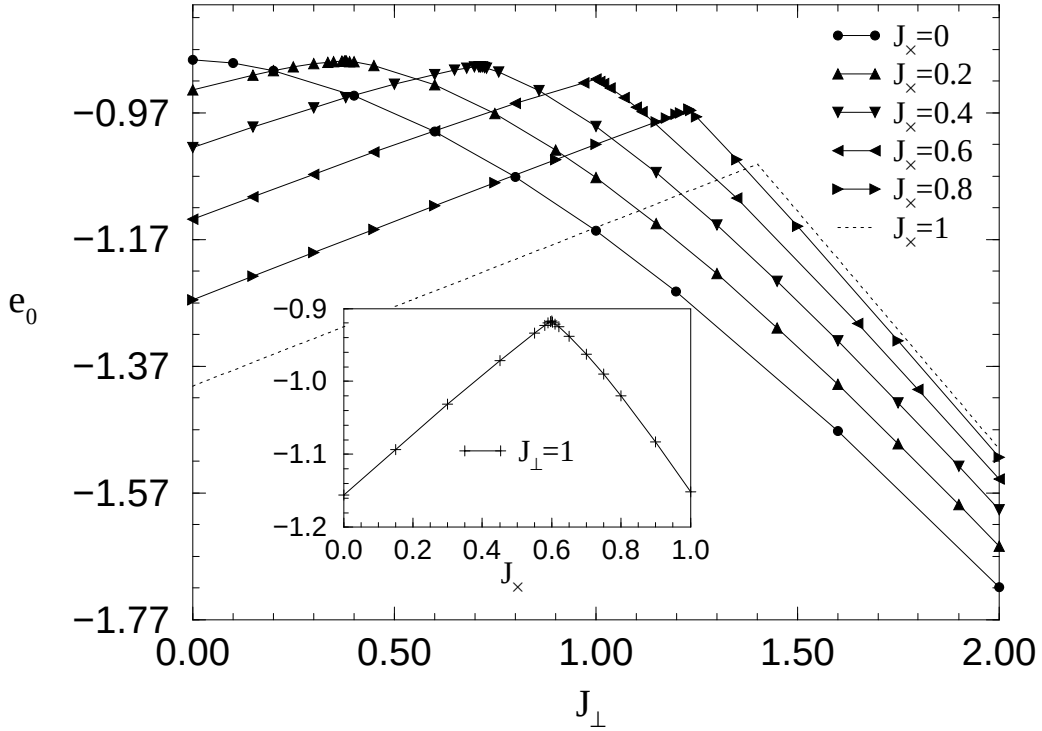

Wang, Figure 4: density of singlets per rung

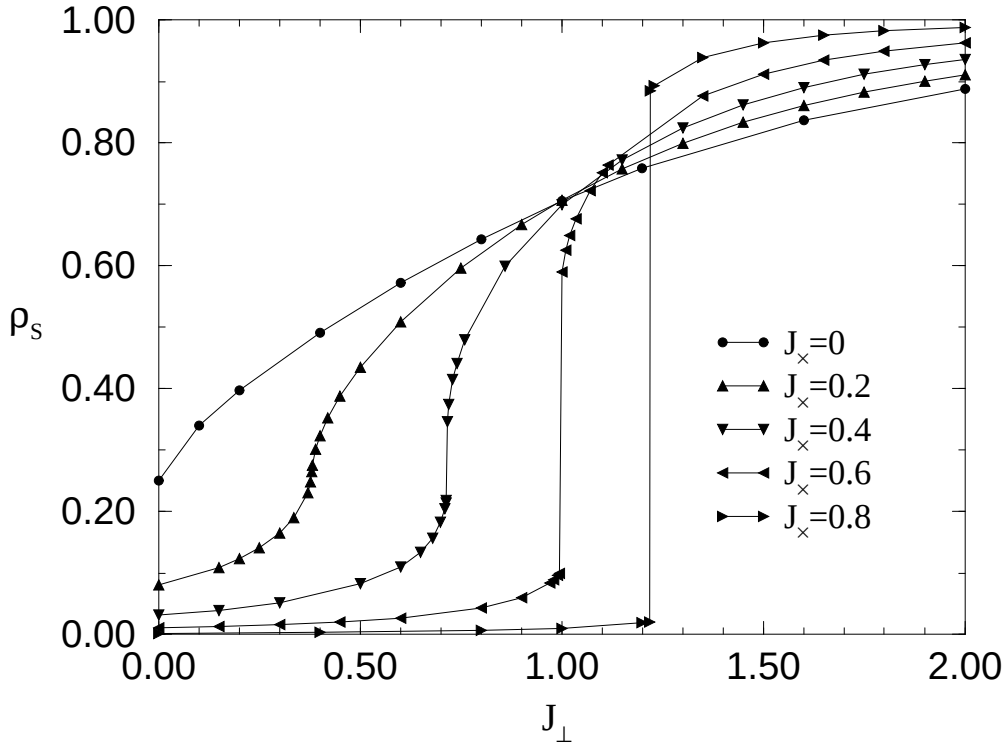

# Wang, Figure 5: low−lying excitations

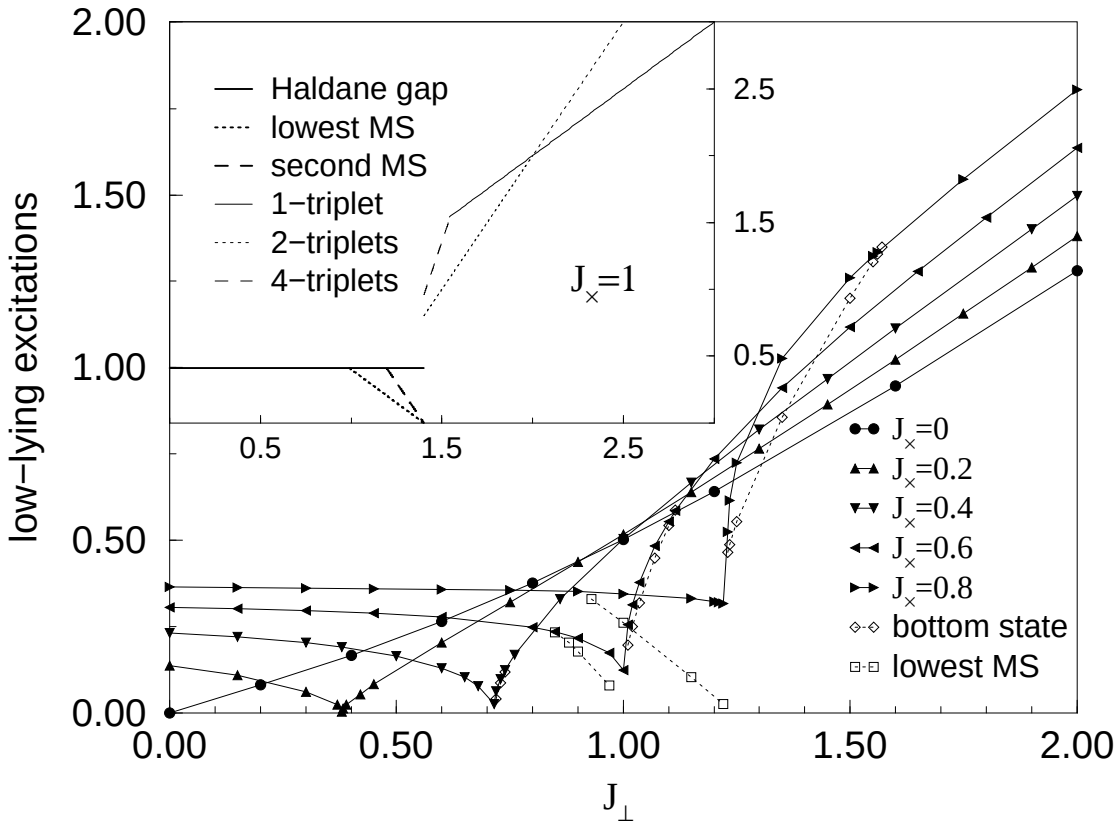

# Wang, Figure 6: spin gap